

Automatic Analysis of Emulsion Chambers Using the Image Scanner

M. Shibata¹, H. Kobayashi¹, Y. Katayose¹, N. Hotta², S. Ozawa², T. Saito³, K. Izu⁴, and S. Ayabe⁵

¹Department of Physics, Yokohama National University, Yokohama, Japan

²Faculty of Education, Utsunomiya University, Utsunomiya, Japan

³Tokyo Metropolitan College of Aeronautical Engineering, Tokyo, Japan

⁴Institute for Cosmic Ray Research, University of Tokyo, Kashiwa, Japan

⁵Department of Physics, Saitama University, Saitama, Japan

Abstract. A new method of emulsion chamber analysis is developed using image scanner. We present the details of the new techniques and some results applied for Tibet hybrid experiment(M.Amenomori et al. 1999) to study primary cosmic-ray composition around 10^{15} eV by observing high energy gamma-families in coincident with air showers. Methods of background reduction, detection of electromagnetic cascade showers and energy determination in the emulsion chamber analysis are presented. The results show that the image scanner can be used as a powerful tool for automatic analysis of emulsion chambers.

1 Introduction

The emulsion chamber is widely used as a powerful detector of high energy gamma-rays with good spacial and energy resolution, however, the scanning of X-ray films by naked eyes requires large manuscript work and regarded as a main defect, especially when we try to observe very high-energy cosmic rays with large exposure area which is needed because of low flux of cosmic rays in high energy region. A solution to overcome this difficulty is to develop an automatic scanning system of X-ray films. If such system is successfully developed, one may expect an exploration of new energy range or new physics.

Recently, the image scanner controlled by the computer becomes available within reasonable cost and applicable for the detection of cascade showers recorded on the X-ray films used in the emulsion chamber.

Basic informations given by the image scanner are three variables, namely, position (x,y) and transparency z which can be related to the optical density D of the shower spots to be used for the energy determination of cascade showers. Another information required in the analysis of emulsion chamber is the incident direction of the parent gamma-rays. We examined the shape of shower spot to determine the incident direction. Details of the treatment of optical density, background reduction, detection of shower spot and determi-

nation of incident direction are described in following sections.

2 Method of Analysis

2.1 Scanner System

Main profiles of the image scanner used in our analysis are as follows.

1. Maximum size of measurable area : 290mm \times 420mm
2. Resolution : 600 dpi (dots/inch)
3. Transparency range : 12bits (0-4095)
4. Graphic data format : TIFF

One sheet of type 200 X-ray film (40cm \times 50 cm) is divided into 2 parts due to limited scanning area. The pixel size is 42.3 μ m \times 42.3 μ m. It takes about 30 minutes to scan one sheet. The recorded data size is 270MB for one sheet of film.

2.2 Optical Density

The image scanner provides us the transparency 'z' as a function of the pixel position (x, y), where $z=4095$ means completely transparent and $z=0$ means completely dark. We examined the relation between z and optical density d measured by photometer using a sample film which has artificial density steps. The result is shown in Fig.1 together with a function

$$d(z) = a - b \log_{10} z, \quad (1)$$

where $a = 7.08, b = 1.94$ are the fitting parameters.

Since the optical density d for the uniform density is defined as

$$d = -\log_{10} \frac{i}{i_0}, \quad (2)$$

where i_0 and i denote the incident light intensity and the penetrating light intensity through the target, respectively. We

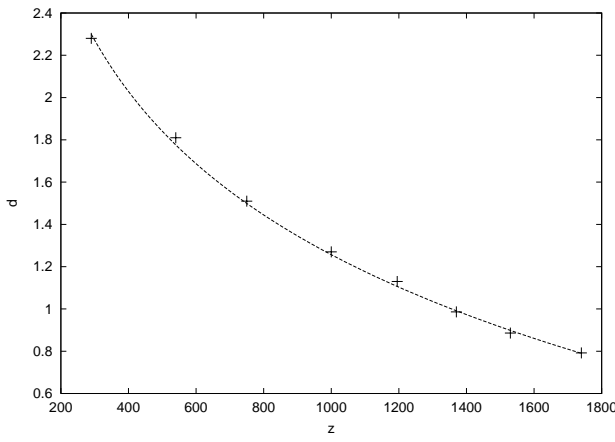


Fig. 1. Relation between optical density d and transparency z

define the spot density D within a finite slit size by following formula as a function of z .

$$\begin{aligned} D(z) &= -\log_{10} \frac{I}{I_0} \\ &= -\log_{10} \frac{\sum_{k=1}^n i_k}{\sum_{k=1}^n i_0} \\ &= -\log_{10} \left[\frac{1}{n} \sum_{k=1}^n 10^{-d_k(z)} \right], \end{aligned} \quad (3)$$

where summation runs over $n = 5 \times 5$ pixels ($211.5 \mu\text{m} \times 211.5 \mu\text{m}$) taking into account of that the slit size of $200 \mu\text{m} \times 200 \mu\text{m}$ is used as an appropriate slit size for the measurement of the spot density of cascade showers in current emulsion chamber experiment.

2.3 Background Subtraction

The local background density B is derived averaging over crossing lines of length of 200 pixels with rejection of large deviation ($> 3\sigma_B$, where σ_B denotes the standard deviation of B). We reject some local areas when B is greater than $< B > + 3\sigma_{< B >}$ where $< B >$ denotes the average of local background density over whole film area. This procedure can reduce the noisy area of film edge with large background radiation and some other parts with heavy noise.

We define net density d_{net} for each pixel as follows.

$$d_{net} = d - B. \quad (4)$$

The net optical density of shower spot with finite slit size D_{net} is defined in the same manner and expressed with use of equations (2) and (3) as follows.

$$D_{net} = D - B = -\log_{10} \left[\frac{1}{n} \sum_{k=1}^n 10^{-d_{net,k}} \right]. \quad (5)$$

2.4 Detection of Shower Spots

The detection of shower spots is made by the boundary following method using the critical net density $d_c = 0.12$. This procedure enables us to find the position of boundary pixels surrounding a spot area with net pixel density greater than d_c . Thus obtained spots, however, still consist of a lot of noises,

for example, about 5000 spots are detected from a sheet of X-ray film while we can recognize by naked eye scanning that 40 are signals among them and others are noises. There are many kind of causes of the origin of the noises. They are, for instance, the contamination of the radioactive isotopes in the film material or the lead plates, the spots formed by the pressure which can be attributed to the small stones mixed up during the construction of the chamber, dirt or damages attached while development of films and so on. These spots can be easily identified as noises by naked eye scanning, but the image scanner picks up them faithfully.

2.5 Noise Reduction

Noise reduction is made by imposing various conditions which are based on the characteristics of the structure of cascade showers. We first apply following three conditions on the global structure of detected spots.

1. We reject those spots with $D_{net} < 0.12$.
2. Elliptic curve fitting is made for each detected spot and we reject those with too large residuals (residual/point > 4 pixels) or too large zenith angle derived from equation (6) ($\tan \theta > 2$).
3. It is imposed that the peak density d_{peak} among 5×5 pixels should be greater than $1.2D$ where D is the net density of the spot in order to reject structure-less spots.

Since the nuclear emulsion is coated on both side of acrylic film-base of thickness $200 \mu\text{m}$, two circular spots are formed neighboring by a certain small distance defined by incident zenith angle of gamma rays. We can approximate the shape of these two overlapping spots as an ellipse as shown in Fig. 2. The direction of longer axis of elliptic curve corresponds to the azimuth angle ϕ of the shower axis, while the length of longer and shorter elliptic axis can be related to the zenith angle θ by following approximation formula.

$$T \tan \theta + \frac{2b}{\cos \theta} = 2a, \quad (6)$$

where T denotes the thickness of film base, $2a$ and $2b$ denote the length of longer and shorter elliptic axis, respectively.

Above mentioned criteria can reduce the number of spots to less than half without rejecting the signals, however, there still remains large number of noise spots having similar global structures to signals.

Further investigation was made to find the difference of fine structure of the density distribution between signals and noises by distinguishing them by naked eye scanning. Following three features of fine structure are compared between signals and noises, in which different characteristics are expected since most of noises have irregular density distribution.

1. The pixel density distribution is approximated by two dimensional gaussian distribution,

$$\rho(x, y) dx dy = a \exp \left[-\frac{x^2 + y^2}{b} \right] dx dy, \quad (7)$$

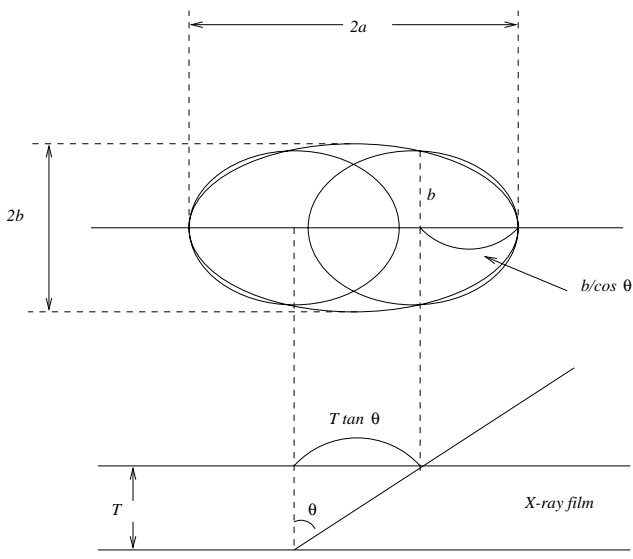


Fig. 2. Elliptic approximation of shower spot

where the parameter b is proportional to the dispersion of the lateral structure.

2. The dispersion of d distribution σ_d^2 is examined as a function of $\sum d$.
3. The dispersion of $d \times r$ distribution σ_{dr}^2 is examined as a function of $\sum d$.

Those features show quite different distributions between signals and noises as expected. The parameter b in eq.(7) is widely distributed for noise spots while that of signals distributes in limited area. Both of σ_d^2 and σ_{dr}^2 for noise spots are about 4 times greater than that of signals in average.

In each of above mentioned features, one can find no signals in half plane of the scatter plots divided by average line as a function of $\sum d$. as shown in Fig3. for σ_{dr}^2 . Therefore

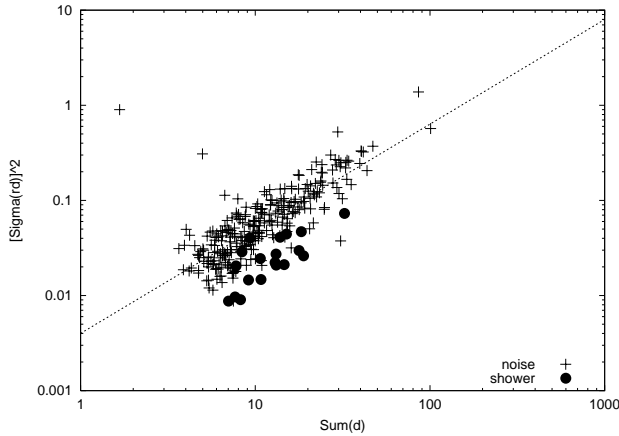


Fig. 3. Scatter plots of $\sigma^2(rd)$ vs. $\sum d$

this region can be used for the noise reduction. After imposing those fine structure criteria, most of noise spots are reduced and most of shower spots remain. An example of

data processing for one sheet of film is listed in following table.

detected spots	5218
reduction by global structure condition	3250
reduction by fine structure condition	1901
remained spots	67

Table 1. Example of data reduction.

The consistency with naked eye scanning in the above example was examined and summarized as follows.

	scanner	naked eye scanning
shower spots	55	59
noise spots	12	-
total	67	59
coincident shower spots	41	
showers by scanner only	14	-
showers by eye scan only	-	$10(D > 0.12), 8(D < 0.12)$

Table 2. Example of detected spots.

2.6 Detection Efficiency

To obtain systematic detection efficiency, the matching of the shower spots detected by the scanner and naked eye scanning are examined carefully using 5 blocks of emulsion chambers. The result is shown in Fig.4 as a function of net density D , where efficiency is defined as the ratio of scanner events to eye-scan events. The efficiency reaches greater than 90% at $D=0.23$ although some of large spots are still missing. The reason of missing large spots is mainly due to neighboring of shower spots with close distance which are regarded to have unfavorable shapes to be signals. It will be improved introducing another algorithms to pick up these spots.

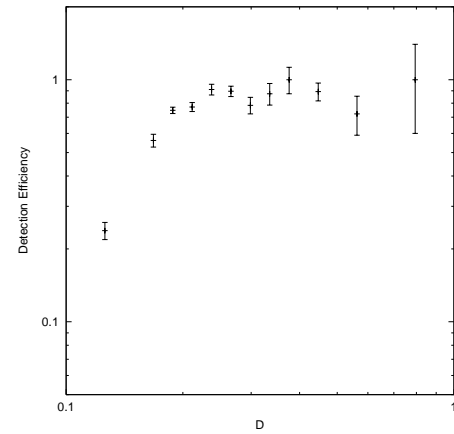


Fig. 4. Detection efficiency of shower spots for net density $D > 0.12$

2.7 Energy Determination

2.7.1 Net Density of Shower Spots by Scanner

The correlation of the net density obtained by the scanner with that of the photometer is shown in Fig.5, where the agreement is satisfactory to be used for energy determination by transition curve fitting. An example of transition curve is

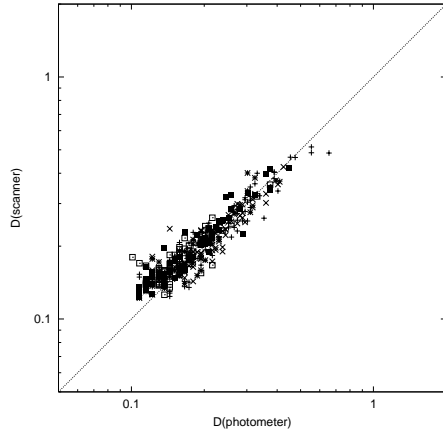


Fig. 5. Comparison of optical densities obtained by photometer and scanner.

shown in Fig.6.

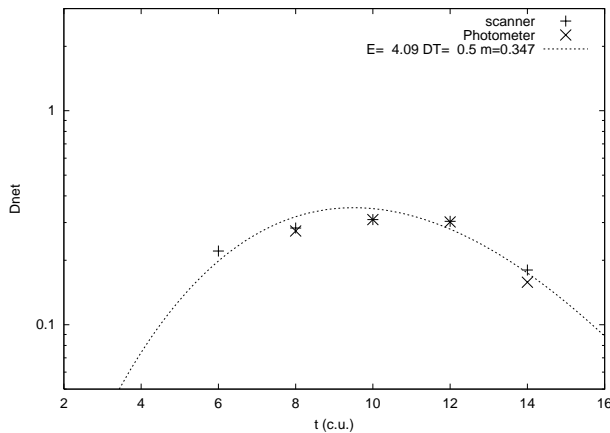


Fig. 6. An example of transition curve compared with photometric method.

2.7.2 Energy Resolution

The ratio of $D(\text{scan})$ to $D(\text{photo})$ distribution leads to relative error being less than 10% in density range of $D > 0.12$ as shown in Fig.7

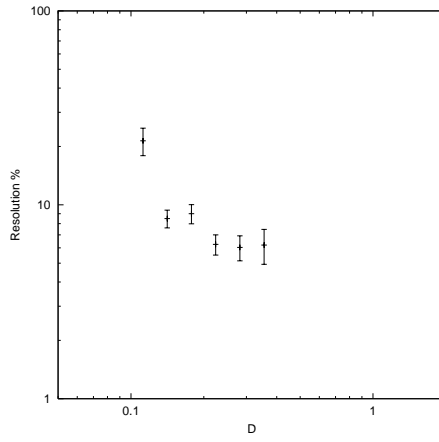


Fig. 7. Relative accuracy of net density between photometer and scanner.

1. The transparency data from the image scanner can be converted to the photometric density by eq.(1).
2. Method of background subtraction and noise reduction are functioning almost sufficiently except the problem of missing neighboring spots.
3. The detection efficiency of shower spots by scanner is greater than 90% in net density range $D_{net} > 0.12$.
4. The energy determination can be done with use of the net density defined in this paper with relative error being less than 10% to the photometric method.
5. The incident direction of showers can be estimated from shape of the spots, however, the efficiency of this process is not discussed yet in present work.

The results described here indicate high possibility to utilize the image scanner for the emulsion chamber analysis.

Acknowledgements. This work is supported in part by Grants-in-Aid for Scientific Research.

References

M.Amenomori, et. al. *27th ICRC OG 1.2.31 2001*, Volume 3, p211, Salt Lake City, USA, 1999

3 Summary

A new method of the emulsion chamber analysis using the image scanner is described. Main conclusions are as follows.